



# Shallow Salt Marsh Tidal Ponds—An Environment With Extreme Oxygen Dynamics

Ketil Koop-Jakobsen<sup>1\*</sup> and Martin S. Gutbrod<sup>2</sup>

<sup>1</sup> MARUM—Center for Marine Environmental Sciences, University of Bremen, Bremen, Germany, <sup>2</sup> Precision Sensing GmbH, Regensburg, Germany

## OPEN ACCESS

### Edited by:

Fereidoun Rezanezhad,  
University of Waterloo, Canada

### Reviewed by:

Amanda C. Spivak,  
University of Georgia, United States  
Hollie Emery,  
Harvard University, United States

### \*Correspondence:

Ketil Koop-Jakobsen  
kjakobsen@marum.de

### Specialty section:

This article was submitted to  
Biogeochemical Dynamics,  
a section of the journal  
Frontiers in Environmental Science

**Received:** 16 May 2019

**Accepted:** 04 September 2019

**Published:** 09 October 2019

### Citation:

Koop-Jakobsen K and Gutbrod MS  
(2019) Shallow Salt Marsh Tidal  
Ponds—An Environment With Extreme  
Oxygen Dynamics.  
*Front. Environ. Sci.* 7:137.  
doi: 10.3389/fenvs.2019.00137

In marshes, tidal ponds are increasing in number and areal coverage. Getting a better understanding of their unique biogeochemistry is a prerequisite for foreseeing their future role in salt marsh ecosystems. Using *in situ* microprofiling, this study investigated the spatiotemporal dynamics of O<sub>2</sub>, pH, and CO<sub>2</sub> in shallow salt marsh tidal ponds in the summer time. High benthic photosynthetic activity, fueled by CO<sub>2</sub> from the sediment, resulted in steep vertical O<sub>2</sub> gradients at the sediment-water interface, increasing from anoxia to extremely supersaturated peak concentrations up to 886 ± 139 μmol L<sup>-1</sup> (391% atmospheric O<sub>2</sub> saturation) over a short distance of 6 mm. These characteristic peaks developed even at low light conditions down to 150 μmol photons m<sup>-2</sup> s<sup>-1</sup> photosynthetically active radiation (PAR). The oxygen gradients were restricted to the layer of benthic microalgae on the sediment surface and did not extend into the water column, which was well-mixed throughout the day showing no vertical variation. The benthic photosynthesis and respiration controlled the oxygen concentration in the water column, creating net supersaturated conditions during the day and hypoxic conditions at night. The tidal ponds were generally well-buffered showing only attenuated pH fluctuations ranging from 6.2 to 7.3, and no persistent gradients built up, despite the high photosynthetic activity at the sediment water interface. CO<sub>2</sub> accumulated in the sediment and was present in the water column during the morning hours, but depleted in the afternoon due to the high photosynthetic uptake. Tidal ponds also experienced event-driven changes in their biogeochemistry. Sea foam developed on the water surface during the day and accumulated on one side of the pond blocking light penetration and lowering oxygen concentrations under the foam. Inundation at high tide caused a short-lived temporal variation in O<sub>2</sub> and pH, which was restricted to the time of the flood. As the flooding water receded, the preceding O<sub>2</sub> and pH conditions were immediately restored. Altogether shallow tidal ponds comprise a marsh habitat with distinctive spatiotemporal oxygen dynamics driven by benthic photosynthesis and respiration, which differ from the surrounding vegetated marsh, and could drive changes in salt marsh biogeochemistry in response to increased pond coverage.

**Keywords:** O<sub>2</sub>, CO<sub>2</sub>, pH, optode, salt marsh, microprofiling, benthic microalgae (BMA), Plum Island Estuary

## INTRODUCTION

Tidal ponds, also referred to as tide pools or potholes, are naturally occurring in salt marshes, creating a mosaic of permanently inundated ponds with bare sediment on the otherwise vegetated salt marsh platform (Harshberger, 1916; Adamowicz and Roman, 2005). Tidal ponds are widespread on the marsh platform occupying typically around 5–15% of the total marsh area (Adamowicz and Roman, 2005; Millette et al., 2010; Wilson et al., 2014), but areal coverages up to 60% has been observed (Schepers et al., 2017). The ponds have an important ecological function as shelter, feeding ground, and spawning area for a large variety of fish, shellfish, and crustaceans (Smith and Able, 1994, 2003; Raposa and Roman, 2001; Allen et al., 2017), and play a significant role supporting fish production in the coastal area (Mackenzie and Dionne, 2008).

Salt marsh tidal ponds constitute a unique habitat characterized by rapid fluctuations in  $O_2$ , temperature and salinity, which can reach extreme levels over a day-night cycle (Smith and Able, 2003). The ponds can be very shallow, down to 3–5 cm. The surrounding marsh vegetation provides little shading from direct exposure to sunlight, which causes the water temperature to increase significantly during hot summer days and salinity to increase in response to high evaporation (Lillebø et al., 2010). A diverse and highly specialized microbial community inhabits the sediment surface (Kearns et al., 2017), and benthic microbial mats dominated by cyanobacteria can form in the summer time (Harshberger, 1916; Ruber et al., 1981). Consequently, there is high benthic photosynthetic  $O_2$  production during the day, and a high sediment  $O_2$  demand caused by microbial respiration and reoxidation of reduced compounds, which leads to marked daily  $O_2$  fluctuations (Ruber et al., 1981).

Under warm and sunny summer conditions, the water column in tidal ponds becomes supersaturated with  $O_2$  during the day, and high respiratory activity results in a depletion of  $O_2$  at night, where the water column can reach hypoxic conditions (Smith and Able, 2003; Lillebø et al., 2010; Baumann et al., 2015; Spivak et al., 2017). This makes harsh living conditions for the organisms that inhabit or get trapped in the tidal ponds after the receding tide. In contrast, the tidal pond water is well-buffered, and pH does not reach extreme values, but fluctuates daily in a range from 7 to 8.5 in the summer months (Lillebø et al., 2010; Baumann et al., 2015; Kearns et al., 2017). Previous studies of daily variations of  $O_2$ , pH, and temperature were primarily conducted as point-measurement in the water column, following the temporal variation over the course of the day. However, *in-situ* data about the gradients, which may build up within this shallow ecosystem, and their spatial and temporal dynamics are lacking, and the causes of these extreme oxygen dynamics are not fully understood.

Therefore, we investigated both the daily temporal and spatial dynamics of  $O_2$ , pH, and  $CO_2$  in shallow salt marsh tidal ponds, highlighting the development of gradients across the sediment-water interface. Using an automated profiling system with needle optodes, high resolution vertical profiles of  $O_2$ , pH, and  $CO_2$  were measured from the air-water interface, through the water

column and into the sediment, exploring the daily variation in vertical gradients and their dependence on light exposure. The investigations were conducted *in situ* and under controlled light conditions in the laboratory.

## METHODS AND MATERIALS

### Study Site

The investigation of shallow salt marsh tidal ponds was conducted in the high marsh of the Plum Island Estuary, MA, USA ( $42^{\circ}44'19''N, 70^{\circ}50'48''W$ ; **Figure 1A**). Three closely located soft-bottomed tidal ponds were investigated (**Figure 1B**). The bottom of the tidal ponds was characterized by a thick layer of photosynthesizing benthic microalgae (**Figure 1C**). The ponds, which are located on the marsh platform, have an area between  $\sim 30$  and  $100\text{ m}^2$ , and a shallow water-depth ( $<10\text{ cm}$ ) (**Figures 1D–F**).

### Experimental Design

The overall scope was to elucidate the daily spatiotemporal variations of  $O_2$ , pH, and  $CO_2$  in shallow salt marsh tidal ponds and to resolve the role of light as a controlling factor. A series of five investigations were designed (**Table 1**). To investigate the spatial variation, vertical profiles were measured with high spatial resolution using an automated needle optode microprofiling device. To account for the daily variation in the profiles, these measurements were conducted in the morning, afternoon, and at night. The impact of light on the spatial variation was investigated on cores from the field in a laboratory-study under controlled light regimes. To further evaluate the temporal variation, a 24 h time-series measurement was conducted in the same pond at a fixed position in the water column with high temporal resolution. Spatial variations within a pond and the influence of sea foam was studied in detail in a forth experiment, and in order to account for differences among different tidal ponds, profiling was conducted consecutively in three independent but closely located ponds within a short timeframe.

All *in situ* measurements were conducted in July 2018 on days with clear skies, where the tidal ponds were directly exposed to sunlight. All laboratory measurements were conducted in July 2017. The investigations focussed primarily on oxygen, which was measured in all investigations, whereas pH and  $CO_2$  were only measured in selected studies (**Table 1**).

### Experimental Set-Up

The experimental set-up is shown in **Figure 2**.  $O_2$ , pH, and  $CO_2$  profiling was conducted using a novel optode microprofiling device from PreSens GmbH (Germany, [www.presens.de](http://www.presens.de)) with an Automated Micromanipulator (AM), needle-type optodes for measurements of oxygen (PM-PSt7), pH (PM-HP5), and  $CO_2$  (PM-CDM1 prototypes), respectively. The sensors were pre-calibrated by the manufacturer, rendering *in situ* calibrations superfluous, which was an advantage, especially in the dark. Prior to the *in situ* and laboratory investigations, the sensors were tested against a known standard. Corrections were not necessary. For *in situ* profiling, an aluminum stand ( $6 \times 6\text{ cm}$ ) holding the Automated Micromanipulator and sensors, was mounted on 1 m

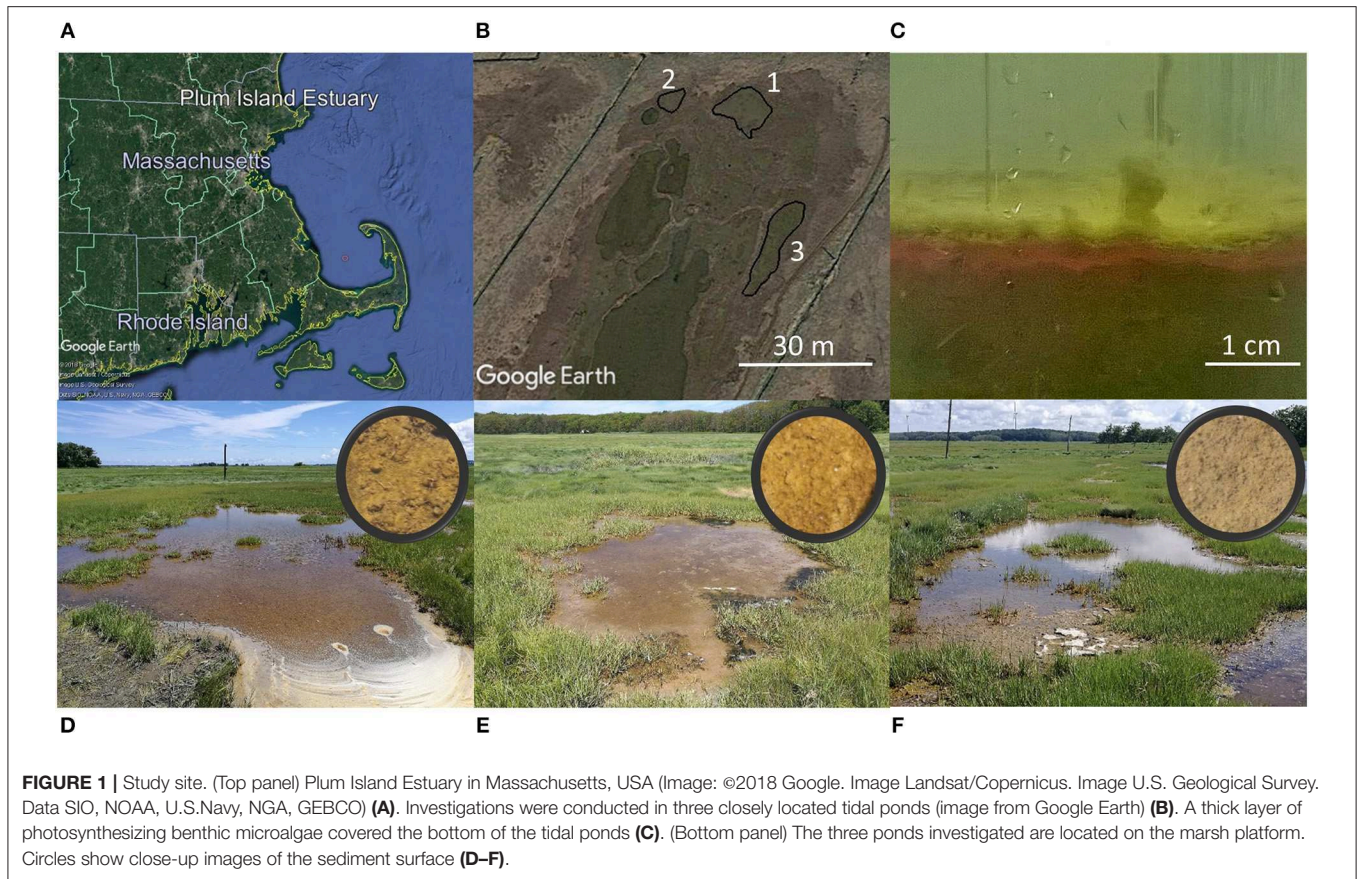


**FIGURE 1 |** Study site. (Top panel) Plum Island Estuary in Massachusetts, USA (Image: ©2018 Google. Image Landsat/Copernicus. Image U.S. Geological Survey. Data SIO, NOAA, U.S.Navy, NGA, GEBCO) **(A)**. Investigations were conducted in three closely located tidal ponds (image from Google Earth) **(B)**. A thick layer of photosynthesizing benthic microalgae covered the bottom of the tidal ponds **(C)**. (Bottom panel) The three ponds investigated are located on the marsh platform. Circles show close-up images of the sediment surface **(D–F)**.

**TABLE 1 |** Overview of *in situ* and laboratory investigations conducted to determine the spatiotemporal variation of  $O_2$ , pH, and  $CO_2$  in shallow salt marsh tidal ponds and the role of light as a controlling factor.

Scope	Conditions	Parameters	Spatiotemporal observations
1 Investigation of spatiotemporal variation over the course of day	<i>In situ</i>	$O_2$ , pH, $CO_2$	Vertical profiles from water surface to anoxic sediment. Measured in the morning, afternoon and night with a resolution of 300–1000 $\mu\text{m}$ .
2 Investigation of light control of spatial variation	Lab.	$O_2$ , pH	Vertical profiles across the sediment-water interface with a resolution of 150–250 $\mu\text{m}$ . Measured under different light regimes: 0, 25, 150, 350 $\mu\text{mol photons m}^{-2}\text{sec}^{-1}$ PAR.
3 Investigation of temporal variation during a day	<i>In situ</i>	$O_2$ , pH	Point measurements in the water column. Time-series - 24 hour. Resolution: 1 $\text{min}^{-1}$
4 Investigation of internal spatial variation of $O_2$ within a pond	<i>In situ</i>	$O_2$	Vertical profiles from water surface to anoxic sediment. Measured around noon with a resolution of 300–1000 $\mu\text{m}$ under various thickness of sea foam.
5 Investigation of spatial variation among different tidal ponds	<i>In situ</i>	$O_2$	Vertical profiles from water surface to anoxic sediment. Measured with a resolution of 300–1000 $\mu\text{m}$ within one afternoon.

long spikes and pushed into the soft sediment of the tidal ponds securely fastening the microprofiling device in a stable position. For laboratory profiling, the aluminum stand was mounted on a heavy base plate.

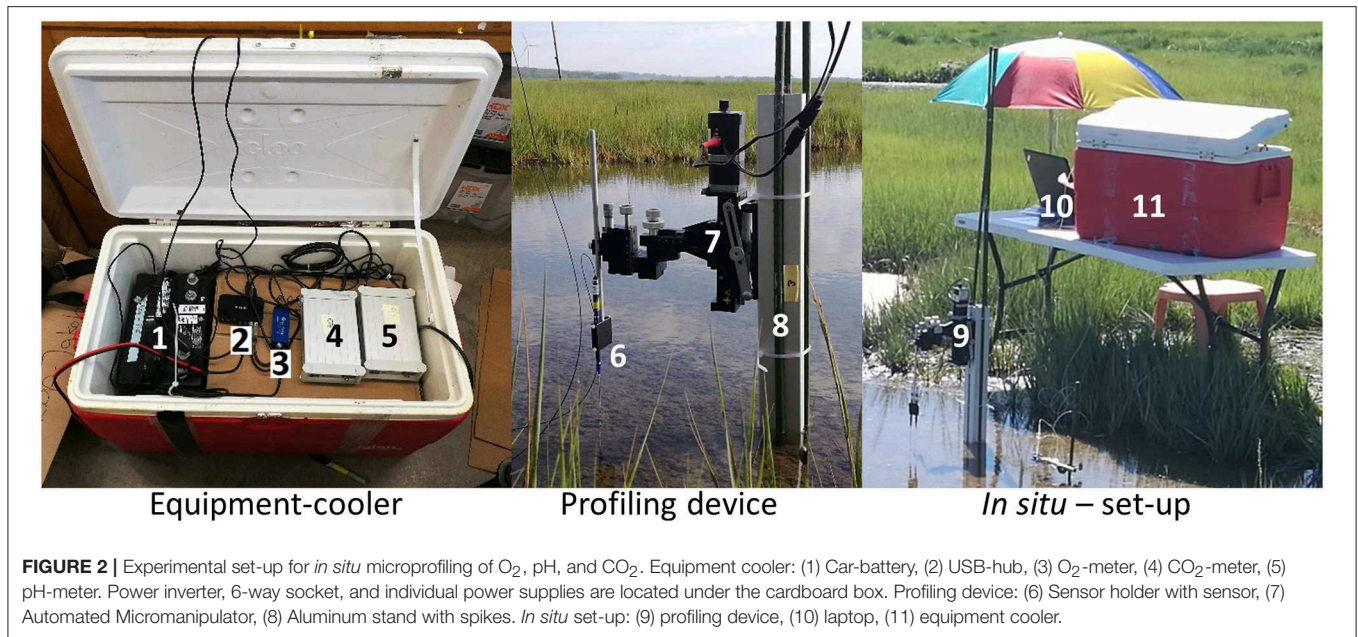
For *in situ* profiling, the needle optode sensors were fastened in a custom-made extended sensor holder allowing the sensor-tips to reach the sediment, while the micromanipulator and its electronics were kept at a safe distance from the water. All other electronic components were packed inside a cooler for protection

from sun, rain, wind and sea-spray, and placed on a table out of tidal range. A cardboard box inside the cooler functioned as a shelf, and as a humidity buffer preventing condensation directly on the equipment during the morning hours.

The system was operated from a laptop and powered by a car-battery with a DC-AC power inverter (12–110 V).

Light and temperature in the water-column was measured with a HOBO Pendant® Temperature/Light Datalogger. Furthermore, light data of the photosynthetically active radiation





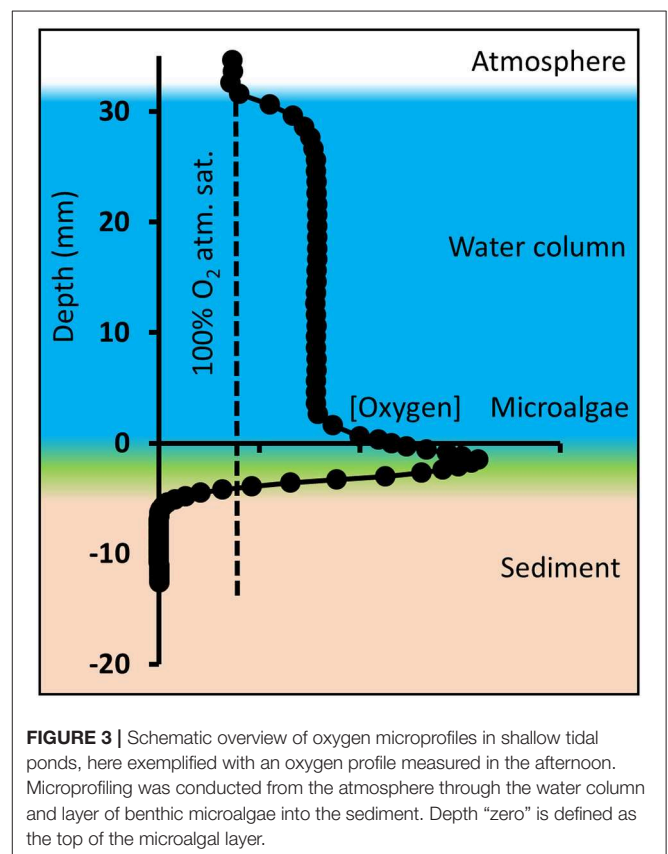
(PAR) was received from a nearby weather station (PIE LTER *Marshview Farm* weather station). Salinity measurements were performed using a refractometer.

## Profiling

*In situ* vertical profiles were measured from the water-air interface, through the water column, and into the sediment until stable anoxic conditions were reached (Figure 3). The resolution was adjusted to the O<sub>2</sub> variability, measuring with 1,000 μm-steps through the water column, and 300 μm per step through the sediment-water interface, where the O<sub>2</sub> gradients became steep. Each steady-state profile was conducted within 10–20 min depending on water depth.

In the laboratory, profiling was conducted in sediment cores (Ø: 7 cm) and vertical profiles were measured from ~1 cm above to ~1 cm below the sediment-water interface. The spatial resolution was 500 μm per step through the water column and 150 μm per step through the sediment-water interface. During profiling, the water column was kept in motion by gently letting air stream over the water surface.

Due to a thick layer of fluffy benthic microalgae on top of the sediment (Figures 1C, 3), the transition from water column to sediment was not sharp, and therefore difficult to detect visually. Consequently, the sediment-water interface was defined as the top of the benthic microalgal layer and represents depth “zero,” which was determined visually by lowering the white-colored tip of the needle optode through the water until it reached the top of the algal layer. The actual sediment surface below the microalgae was not visible. In the profile, positive values represent the water column, and negative values represent the sediment including the benthic microalgae layer. This caused the oxygen peaks generated by the benthic microalgae to be located below depth “0” and replicate profiles to differ slightly in height of the water column (Figure 3). Average water column



concentrations, average benthic peak concentrations and oxygen penetration depth was calculated from the profiles. The average concentrations and average pH for the tidal ponds, which are shown in tables in the results section, were calculated from the

average of the profile-values at depth from 1 to 2 cm. Benthic peak O<sub>2</sub> concentrations were calculated as an average of the maximum concentrations measured at the sediment-water interface, and O<sub>2</sub> penetration depth was measured as the distance from the top of the sediment-water interface (“depth 0”) to the depth, where the sediment became anoxic. Conversion between % atmospheric O<sub>2</sub> saturation and molar concentrations (μmol L<sup>-1</sup>) was conducted compensating for temperature and salinity using conversion equations from Weiss (1970). Oxygen fluxes across the diffusive boundary layer (DBL) between the overlying pond water and the sediments were calculated from the linear DBL gradients of the oxygen profiles according to Fick’s first law of diffusion:

$$J = D_0 \times \frac{dC}{dx}$$

Diffusion coefficients (D<sub>0</sub>) of seawater were derived from Broecker and Peng (1974) and compensated for temperature and salinity according to the Stokes-Einstein relation (Yuan-Hui and Gregory, 1974). The fluxes therefore represent the diffusive oxygen fluxes between the water column and the underlying microalgae layer.

## Investigations

**1) *In situ* Investigation of Spatiotemporal Variations of O<sub>2</sub>, pH, and CO<sub>2</sub>.** Replicate O<sub>2</sub> ( $n = 3$ ) and pH ( $n = 2$ ) profiles were measured at different positions within a 30 cm radius in the morning (07:30–09:30), afternoon (14:00–16:00) and at night (00:30–02:30). CO<sub>2</sub> sensors are sensitive to sulfide, which is present in the sediment pore water, hence CO<sub>2</sub> profiles were only measured a short distance into the sediment and as single profiles.

**2) Laboratory Investigation of Light Control of the Spatial Variations of O<sub>2</sub> and pH.** For investigation of the light dependency of benthic O<sub>2</sub> and pH dynamics, profiling was conducted in sediment cores under different light regimes. Light exposures were set to 0, 25, 150, and 350 μmol photons m<sup>-2</sup> s<sup>-1</sup> photosynthetically active radiation (PAR), respectively, and temperature was fixed at 20°C and salinity at 35‰. To assure equilibrium conditions, the cores were exposed to each light setting for 6 h prior to profiling. Light conditions were measured at the sediment surface with a handheld light meter (LiCor LI-250). Sediment cores from the study site were collected by hand using Plexiglas cylinders ( $\phi = 7$  cm). The cores were kept in a growth chamber for 2 days prior to profiling investigation at 20°C with a 12/12 h dark light cycle. The water columns were maintained with water from the pond and aerated with an aquarium pump. There were three independent replicate cores per light treatment ( $n = 3$ ).

**3) *In situ* Investigation of Daily Temporal Variations of O<sub>2</sub> and pH.** For investigation of temporal variation, needle optodes for O<sub>2</sub> and pH were placed in a fixed position at a distance of 2 cm above the sediment-water interface. O<sub>2</sub> and pH were monitored for 24 h at 1-min intervals. The measurements included one tidal inundation.

**4) Internal Spatial Variation of O<sub>2</sub> Within Shallow Tidal Ponds—The Role of Sea Foam.** In the late morning, sea foam

developed on the water surface and accumulated on one side of the pond depending on the wind direction, providing natural light and wind shading of the water column and sediment surface. For investigation of its impact on the spatial internal variation in oxygen distribution, profiles were measured in three locations in the pond with variable foam thickness. A light logger was placed under the foam in order to determine light penetrability to the sediment surface.

**5) Investigation of Spatial Variations Among Independent Tidal Ponds.** In order to investigate the variation between different tidal ponds, replicate O<sub>2</sub> profiles ( $n = 3$ ) were measured in three closely located tidal ponds (Figures 1B,D–F). The ponds were investigated consecutively in the afternoon within the shortest possible time-frame (11:10–14:40) to assure comparable environmental conditions.

## Statistical Analysis

Statistical analysis of differences among time of day (1), light exposure (2), and different ponds (3), respectively, were analyzed statistically using a one-way ANOVA with Tukey’s HSD ( $\alpha = 0.05$ ) *post hoc* tests. The analyses were generated using the Real Statistics Resource Pack software (Release 6.2, www.real-statistics.com). Statistical analyses are limited to the experiments where  $n \geq 3$ .

## RESULTS

**1) *In situ* Investigation of Spatiotemporal Variations of O<sub>2</sub>, pH, and CO<sub>2</sub>.** The tidal ponds had high O<sub>2</sub> dynamics ranging from anoxic conditions inside the sediment to extreme supersaturation. The largest concentration was 1,016 μmol L<sup>-1</sup> (460% atmospheric O<sub>2</sub> saturation) measured at the sediment water interface during the morning hours (Figure 4).

A thick layer of benthic microalgae was present on the sediment surface (Figure 1C) resulting in a marked peak in O<sub>2</sub> and steep O<sub>2</sub> gradients during daylight. The top of the algal layer was defined as “depth zero” in the profiles, and consequently the O<sub>2</sub> peaks were located between 0 and –10 mm depth. The sediments were completely anoxic greater –10 mm depth. The gradients were restricted to the layer of benthic microalgae and their DBL and did not extend into the water column. The benthic O<sub>2</sub> peaks were already established in the morning (07:50) with a concentration of 886 ± 139 μmol L<sup>-1</sup>, and peaks remained in the afternoon, where the oxygen was slightly lower 593 ± 177 μmol L<sup>-1</sup>. At night the peak disappeared as the concentration dropped to 45.9 ± 3.6 μmol L<sup>-1</sup>, at the sediment-water interface. The O<sub>2</sub> penetration depth, measured from the top of the microalgal layer, varied over the course of the day from 10 and 7.6 mm in the morning and afternoon, respectively, to only 1.8 mm at night (Figure 4).

The shallow water column showed little vertical variation in O<sub>2</sub>, pH, and CO<sub>2</sub>. The average water-column O<sub>2</sub> varied over the course of the day. In the morning, the O<sub>2</sub> concentration was close to the atmospheric equilibrium 293 ± 47 μmol L<sup>-1</sup>, but increased rapidly, which was demonstrated in the profiles, where the concentration in the water column increased from ~240 to ~350 μmol L<sup>-1</sup> in the consecutively measured

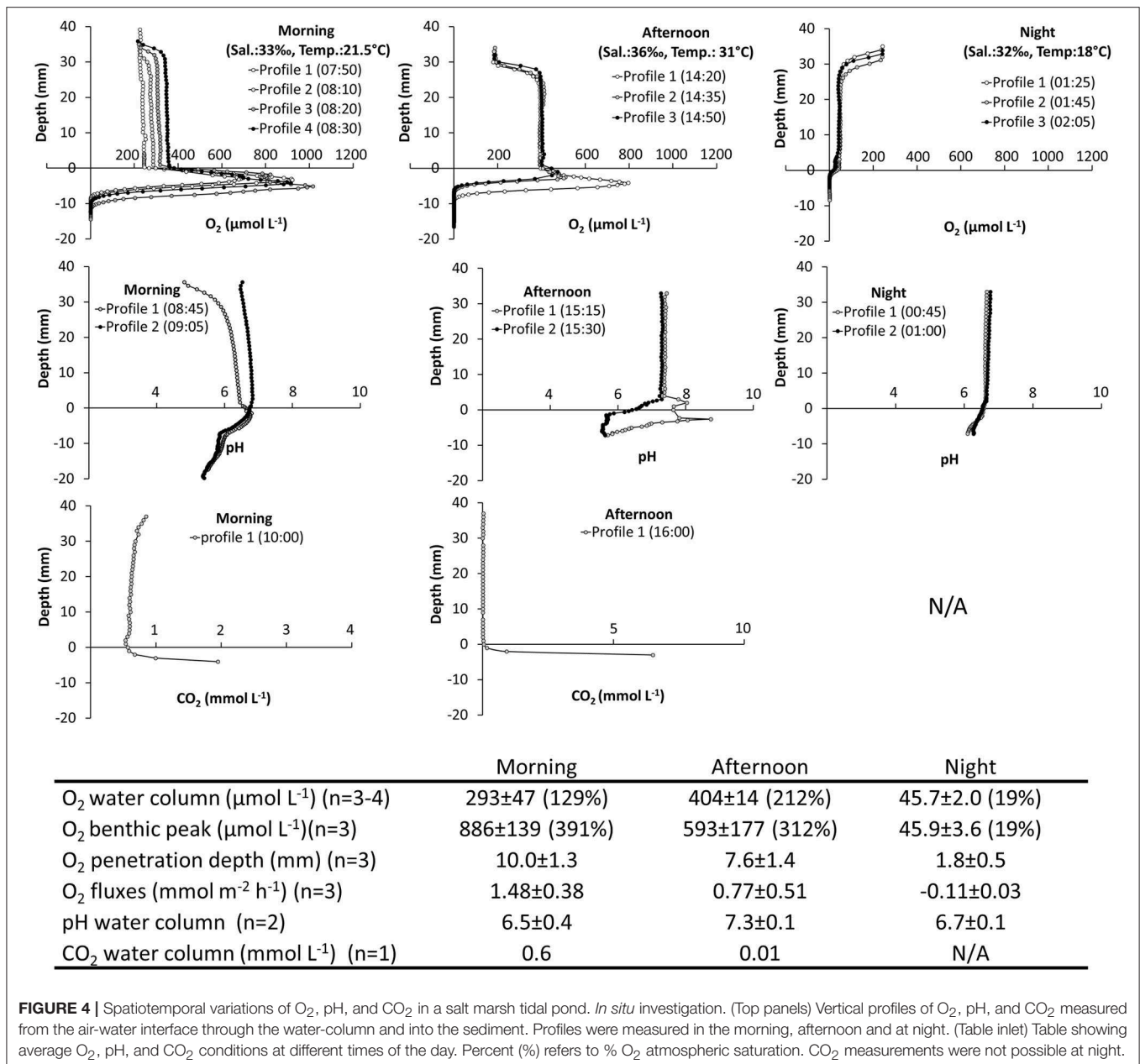


**FIGURE 4** | Spatiotemporal variations of O<sub>2</sub>, pH, and CO<sub>2</sub> in a salt marsh tidal pond. *In situ* investigation. (Top panels) Vertical profiles of O<sub>2</sub>, pH, and CO<sub>2</sub> measured from the air-water interface through the water-column and into the sediment. Profiles were measured in the morning, afternoon and at night. (Table inlet) Table showing average O<sub>2</sub>, pH, and CO<sub>2</sub> conditions at different times of the day. Percent (%) refers to % O<sub>2</sub> atmospheric saturation. CO<sub>2</sub> measurements were not possible at night.

profiles. In the afternoon, the oxygen in the water-column reached a supersaturated level at  $404 \pm 14 \mu\text{mol L}^{-1}$ , which also resulted in an O<sub>2</sub> gradient building up at the water-air interface. At night, O<sub>2</sub> was depleted in the water column to hypoxic conditions at an average of  $45.7 \pm 2.0 \mu\text{mol L}^{-1}$ . O<sub>2</sub> fluxes between the sediment and the water column varied accordingly with net average O<sub>2</sub> fluxes of  $1.48 \pm 0.38$ ,  $0.77 \pm 0.51$ , and  $-0.11 \pm 0.03 \text{ mmol m}^{-2} \text{ h}^{-1}$  in the morning, afternoon and night, respectively. Oxygen fluxes changed by an order of magnitude between day and night, underpinning the strong benthic control on the O<sub>2</sub> content of the shallow water column (Figure 4).

For O<sub>2</sub>, a one-way ANOVA showed significant differences between morning, afternoon and nighttime for water column

concentration ( $F = 104.8, p = 0.00001$ ), O<sub>2</sub> penetration depth ( $F = 41.4, p = 0.0001$ ), and benthic peak concentration ( $F = 35.3, p = 0.0002$ ). *Post hoc* tests (Tukey's HSD  $\alpha = 0.05$ ) showed that water column concentrations in morning, afternoon, and night were all significantly different ( $p \leq 0.007$ ). This was also the case for benthic O<sub>2</sub> peak concentration ( $p \leq 0.05$ ). For O<sub>2</sub> penetration depth night conditions were significantly different from both morning and afternoon ( $p \leq 0.001$ ).

The tidal ponds had a pH environment within the normal range for marine sediments ranging from 5.8 to 8.7 over the course of a day. In the water column, pH was highest in the afternoon ( $7.3 \pm 0.1$ ), and was slightly lower in the morning ( $6.5 \pm 0.4$ ), and at night ( $6.7 \pm 0.1$ ). In the morning, pH varied



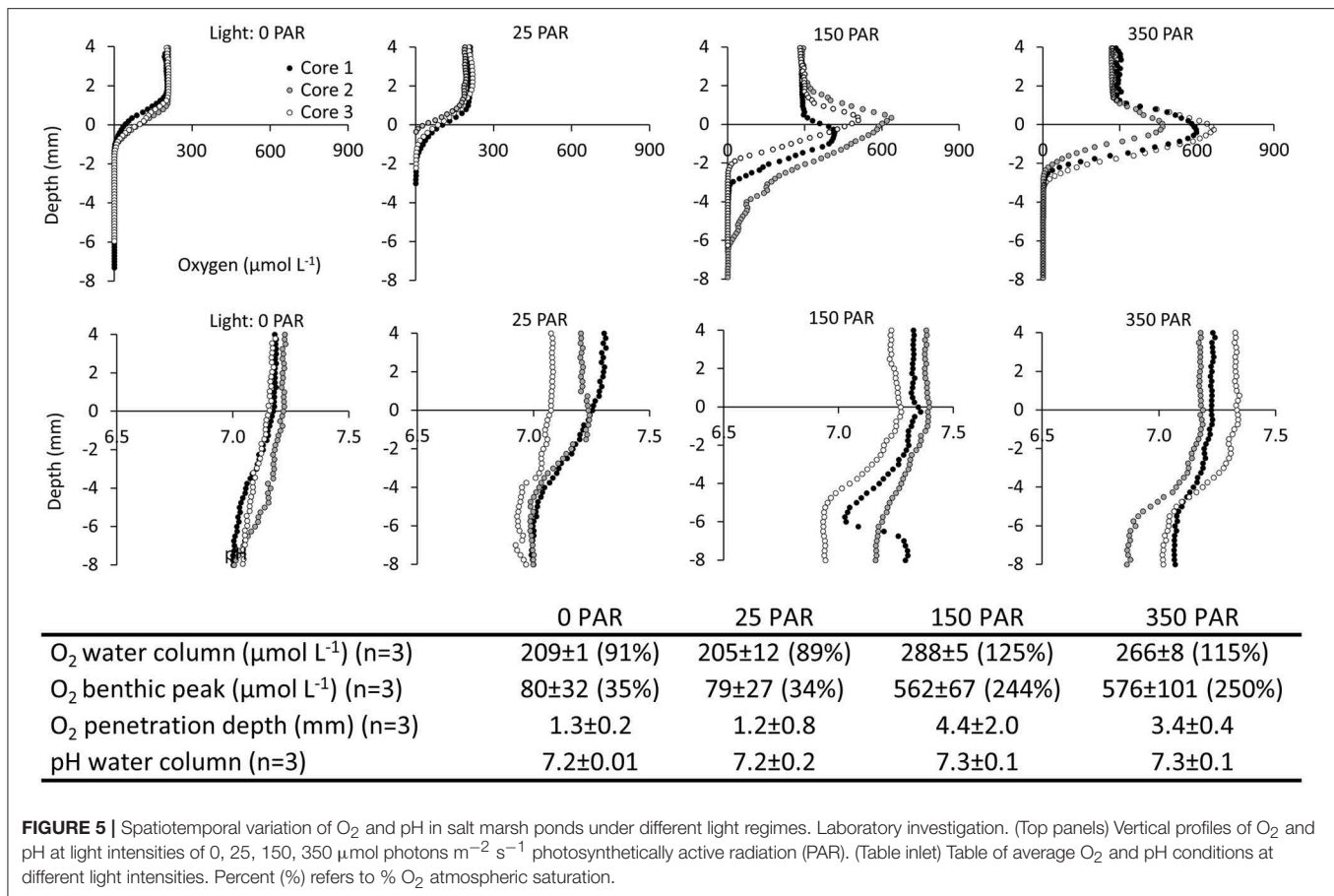


**FIGURE 5** | Spatiotemporal variation of O<sub>2</sub> and pH in salt marsh ponds under different light regimes. Laboratory investigation. (Top panels) Vertical profiles of O<sub>2</sub> and pH at light intensities of 0, 25, 150, 350 μmol photons m<sup>-2</sup> s<sup>-1</sup> photosynthetically active radiation (PAR). (Table inset) Table of average O<sub>2</sub> and pH conditions at different light intensities. Percent (%) refers to % O<sub>2</sub> atmospheric saturation.

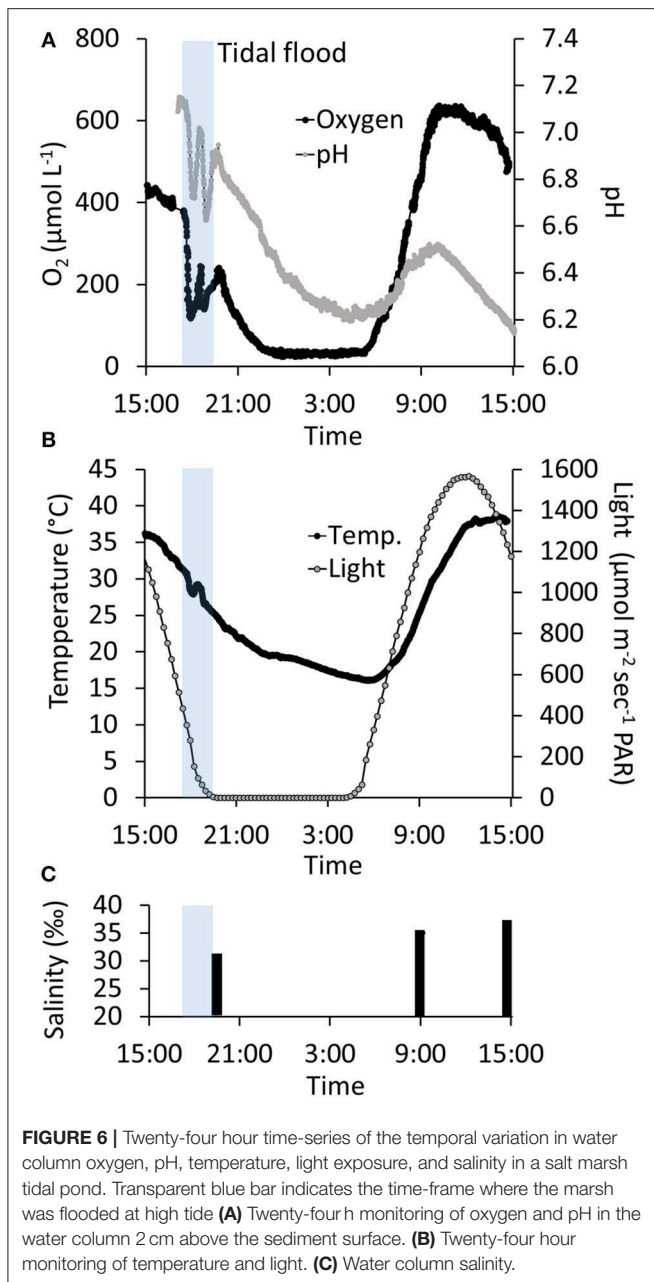
between profiles in the water column, but in the afternoon and at night the profiles were similar. Despite the high benthic microalgal activity, there was no characteristic pattern for pH at the sediment-water interface. In the afternoon, the profiles varied markedly at the sediment surface showing both a peak and decrease in pH. However, in the morning, when the algal activity was highest, there was no corresponding variation in pH. In the water column, the CO<sub>2</sub> profile was vertically stable at a concentration of ~0.6 mmol L<sup>-1</sup> in the morning, but by the afternoon CO<sub>2</sub> was completely depleted. CO<sub>2</sub> accumulated in the sediment showing steep gradients toward the sediment surface. The nighttime CO<sub>2</sub> profile was omitted, due to sensor malfunction. No statistic analyses are available for pH and CO<sub>2</sub>, due to low sample size (Figure 4).

**2) Laboratory Investigation of Light Control of the Spatial Variations of O<sub>2</sub> and pH.** In light (150 and 350 μmol m<sup>-2</sup> s<sup>-1</sup> PAR), oxygen accumulated at the sediment-water interface reaching concentrations of 562 ± 67 and 576 ± 101 μmol L<sup>-1</sup>, respectively. In darkness and at very low light (0 and 25 μmol m<sup>-2</sup> s<sup>-1</sup> PAR), there was no benthic O<sub>2</sub> accumulation, and O<sub>2</sub> concentrations declined across the sediment-water interface and became anoxic within the first millimeters of the sediment. Light had a marked impact on the O<sub>2</sub> penetration depth, which increased from ~1.3 mm in darkness and at very low light (0 and 25 μmol m<sup>-2</sup> s<sup>-1</sup> PAR) to 4.4 and 3.4 mm at 150 and 350

μmol m<sup>-2</sup> s<sup>-1</sup> PAR, respectively (Figure 5). For O<sub>2</sub>, a one-way ANOVA showed significant differences between light exposure treatments for water column concentration ( $F = 78.7, p = 0.000003$ ), benthic peak ( $F = 58.2, p = 0.00001$ ) and O<sub>2</sub> penetration depth ( $F = 5.8, p = 0.02$ ). *Post hoc* tests (Tukey's HSD  $\alpha = 0.05$ ) showed that water column and benthic peak O<sub>2</sub> concentrations in 0 and 25 μmol m<sup>-2</sup> s<sup>-1</sup> PAR were significantly different from 150 to 350 μmol m<sup>-2</sup> s<sup>-1</sup> PAR ( $p \leq 0.0001$ ). For the O<sub>2</sub> penetration depth, 0 and 25 μmol m<sup>-2</sup> s<sup>-1</sup> PAR were only significantly different from 150 μmol m<sup>-2</sup> s<sup>-1</sup> PAR ( $p \leq 0.04$ ).

pH in the water column varied between 7.2 and 7.4. From the sediment surface to a depth of 6–8 mm, pH slowly declined by ~0.2 pH units. Although the O<sub>2</sub> profiles showed a marked photosynthetic activity during light exposure, this activity did not affect pH at the sediment-water interface, and no spatial differences in the pH profiles were observed among different light treatments (Figure 5). For pH no significant differences were found between light treatments ( $F = 0.84, p = 0.5$ ).

**3) In situ Investigation of Daily Temporal Variation.** From mid-afternoon (~15:00), O<sub>2</sub> in the water column decreased from an oversaturated level at 436 μmol L<sup>-1</sup> (241% O<sub>2</sub> atm. sat.) to 33 μmol L<sup>-1</sup> (14 % O<sub>2</sub> atm. sat.) at ~23:00, only interrupted by fluctuations during tidal inundations at ~16:45. The nighttime O<sub>2</sub> concentration remained at this level



throughout the night, and the water column never became anoxic. The  $O_2$  concentration began to increase drastically in the early morning hours starting at 05:20, about 45 min after the break of dawn (04:30). The  $O_2$  concentration increased to reach a maximum of  $638 \mu\text{mol L}^{-1}$  (346%  $O_2$  atm. sat.) at  $\sim 10:00$ , about 3 h before the highest light intensity. The  $O_2$  concentration remained at this level for 1.5 h and subsequently decreased to  $495 \mu\text{mol L}^{-1}$  at 15:00, reaching a level very close to the  $O_2$  concentration at which the measurements began 24 h earlier (Figure 6A).

From mid-afternoon ( $\sim 15:00$ ), pH in the water column decreased from 7.1 to 6.2 in the middle of the night ( $\sim 04:00$ ), only interrupted by fluctuations during a tidal

inundation. Subsequently, pH increased to 6.5, which was reached at  $\sim 10:00$ , after which it began to decrease again and steadily decreased to 6.1 at 15:00 at the end of the time-series measurements (Figure 6A). Temperature showed marked daily fluctuations, ranging from 18 to  $38^\circ\text{C}$  measured at night (03:30) and in the afternoon (14:00), respectively (Figure 6B). Salinity was 32‰ right after the tidal inundation at 19:00. Subsequently, the salinity increased to 35‰ at 09:00 the following morning and reached 37‰ at 15:00 in the afternoon (Figure 6C). During the 24 h monitoring period, there was one inundation at high tide in the late afternoon ( $\sim 16:45$ ). The subsequent high tide 12 h later was too low to reach the marsh platform and the tidal ponds.

$O_2$  and pH were markedly affected by the tidal inundation. On the incoming tide, tidal water was mixed with the pond water column, lowering the oxygen concentration and pH. During the short period at the peak of the tide, where the water movement ceased, the oxygen and pH returned to the conditions before the flood. This pattern was repeated on the outgoing tide leaving a characteristic “W”-pattern in the oxygen and pH time-series (Figure 6). In contrast, the impact of flooding on temperature was negligible (Figure 6).

**4) Internal Spatial Variation of  $O_2$  Within Shallow Tidal Ponds—The Role of Sea Foam.** Oxygen profiles were measured *in situ*; under a thick sea foam layer, under a thin sea foam layer, and in an area with no sea foam, respectively (Figure 7). Water column oxygen was lower under the thick sea foam layer compared to thin sea foam layers and no seafoam (Figure 7). A light logger placed under the foam showed no light penetrability through the thickest layers of seafoam, and a marked reduction of light penetrability under the thin sea foam layer.

**5) Investigation of Spatial Variations Among Independent Tidal Ponds.** All three tidal ponds had similar  $O_2$  concentrations in the water column around  $400 \mu\text{mol L}^{-1}$ , and there were no significant differences between tidal ponds ( $F = 0.12$ ,  $p = 0.88$ ; Figure 8). All tidal ponds showed a peak in  $O_2$  concentration at the sediment water interface. However, the peak concentration differed among tidal ponds ( $F = 10.46$ ,  $p = 0.01$ ), where pond 1 showed significantly larger peaks than pond 2 and 3 (Tukey’s HSD- $\alpha = 0.05$ ,  $p \leq 0.01$ ).

## DISCUSSION

Salt marsh tidal ponds are a unique environment characterized by its distinct light, temperature, salinity and oxygen dynamics during the summer-time (Figures 4, 6–8). In this study conducted in July, oxygen varied daily from hypoxic conditions at nighttime to highly supersaturated concentrations during the daytime (Figures 4, 6) with peak concentrations at the sediment-water interface reaching a maximum of  $886 \pm 139 \mu\text{mol L}^{-1}$



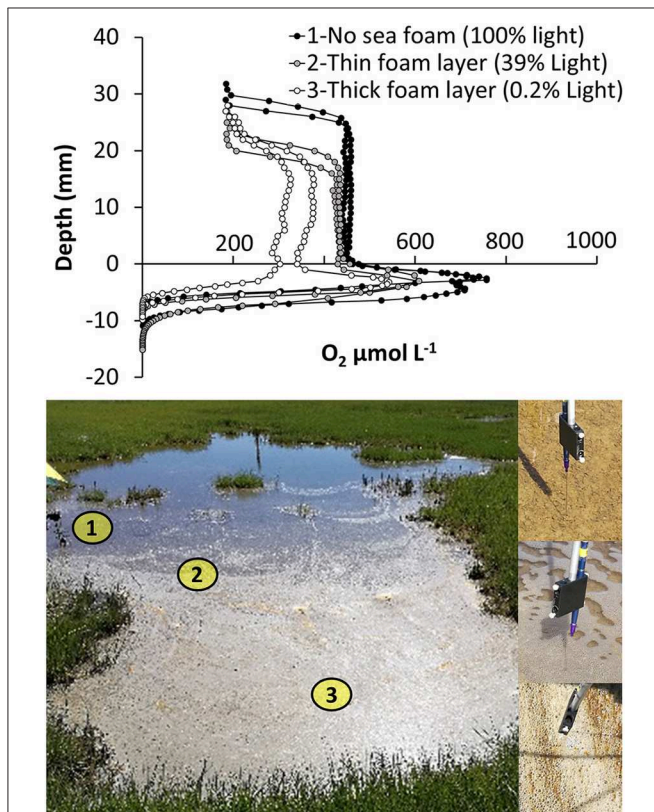


**FIGURE 7 |** Spatial variations in oxygen distribution within a salt marsh tidal pond. Oxygen profiles were measured at three locations with increasing thickness of sea foam and variable light penetrability: (1) no sea foam (65,000 ± 1,000 lux–100% light penetration) (2) a thin seafoam layer (26,000 ± 9,000 lux–39% light penetration), and (3) a thick seafoam layer (150 ± 75 lux–0.2% light penetration).

(391% O<sub>2</sub> atm. sat.) during the morning hours (Figure 4). The temperature swings in the water spanned from 16°C in the nighttime to 38°C in the middle of the day (Figure 6). Due to high evaporation, salinity also increased over the course of the day, especially in the shallowest ponds, where salinities up to 42‰ were observed (Figure 8). Despite these harsh living conditions, tidal ponds provide an important ecological function as a low-tide refuge for endemic salt marsh species (Raposa, 2008; Allen et al., 2017), and various fishes and shrimps were observed in the ponds between tides during these experiments. This study specifically targets shallow marsh tidal ponds with a depth below 10 cm, high light penetrability and domination of benthic microalgae on the sediment surface. In this way, these ponds may share some of the characteristics of salt pannes. However, in contrast to pannes, the water generally remains between tides in these shallow tidal ponds, and thereby they also share characteristics with the deeper ponds in the area.

### Benthic Oxygen Dynamics

A thick layer of benthic microalgae covered the sediment surface and controlled oxygen dynamics in the tidal ponds. The spatial distribution of the microalgae was uneven and occasional wads stretched into the water column (Figure 1C). The benthic algae caused a high net oxygen production and fluxes into the water column in light, and created a thick diffusion limited layer on top of the sediment, where oxygen rapidly accumulated resulting in characteristic peaks at the sediment-water interface during light hours (Figures 4, 5, 7, 8). The opposite situation was present in the nighttime, where the oxygen flux was reversed and oxygen was taken up across the sediment-water interface resulting in a hypoxic water column (Figure 4).

Both the *in situ* profiling (Figure 4) and the light dependency measurements in the laboratory (Figure 5) showed that light

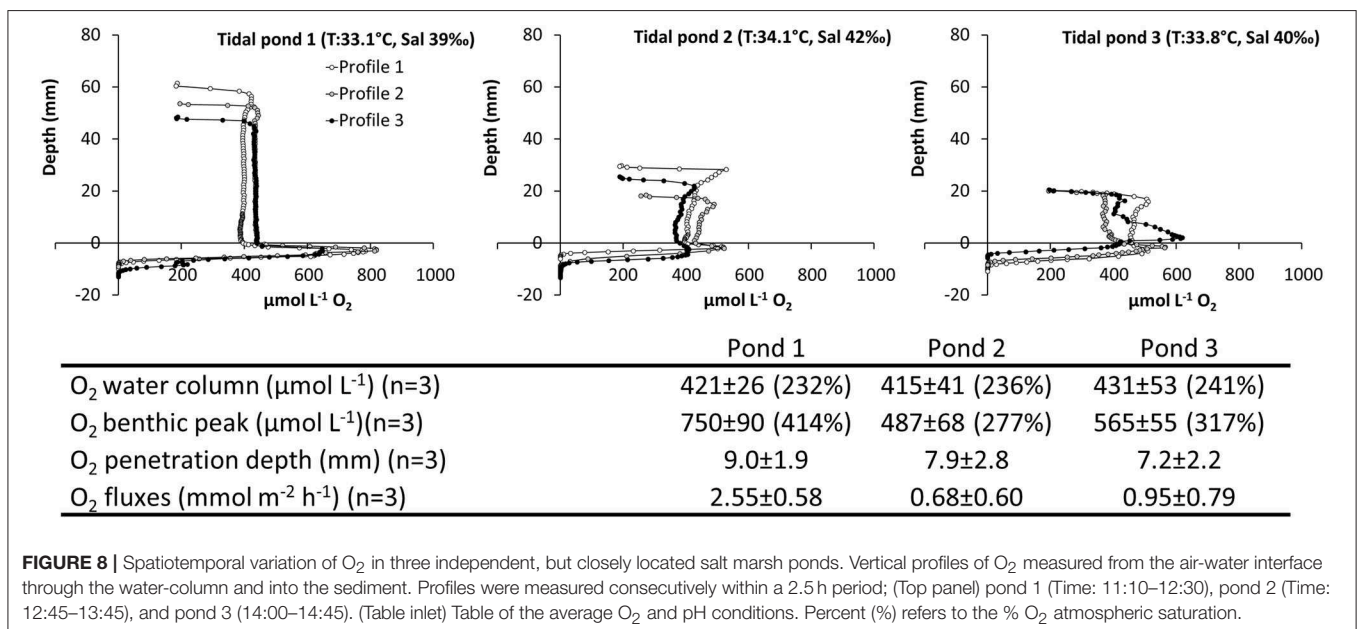


**FIGURE 8 |** Spatiotemporal variation of O<sub>2</sub> in three independent, but closely located salt marsh ponds. Vertical profiles of O<sub>2</sub> measured from the air-water interface through the water-column and into the sediment. Profiles were measured consecutively within a 2.5 h period; (Top panel) pond 1 (Time: 11:10–12:30), pond 2 (Time: 12:45–13:45), and pond 3 (14:00–14:45). (Table inlet) Table of the average O<sub>2</sub> and pH conditions. Percent (%) refers to the % O<sub>2</sub> atmospheric saturation.

controlled the oxygen penetration depth that varied from a few millimeters at night and up to 10 mm in the morning, where the oxygen production was highest. As depth “zero” was the top of the microalgae layer, the oxygen penetration depth represents oxygen penetration through the microalgae layer as well as the sediment. The diminishing gradients at the sediment-water interface were steep, and in the morning, oxygen went from peak concentrations of  $886 \pm 139$  to  $0 \mu\text{mol L}^{-1}$  over a distance of only  $\sim 6$  mm indicating that the sediment has a high oxygen demand (Figure 4).

High photosynthetic benthic oxygen production was present even at low light intensities, and the development of benthic oxygen peaks occurred at light intensities as low as  $150 \mu\text{mol m}^{-2} \text{s}^{-1}$  PAR and did not increase at higher light intensities (Figure 5). This indicates that the benthic microalgae reach their maximum photosynthetic capacity at very low light levels. *In situ*, this light level was reached at  $\sim 06:00$  in the morning, which also coincided with the time where the water column oxygen concentration began to increase rapidly after being low during the nighttime (Figure 6).

The benthic peak oxygen concentration was highest in the morning. In the afternoon, the average oxygen peak was slightly lower (Figure 4). Previous studies have demonstrated photoinhibition of benthic microalgae in salt marshes in full sunlight (Whitney and Darley, 1983), and it is likely to have played a role lowering the afternoon benthic oxygen production. Furthermore, the temperature increased about  $10^\circ\text{C}$  from the morning to the afternoon, which likely increased the microbial oxygen demand, and contributed to the lower peak concentrations. This also markedly lowered the oxygen flux from the sediment surface to the water column.

## Water Column Oxygen Dynamics

Photosynthesis and respiration of benthic microalgae and sediment determined the oxygen saturation state of the bulk water column, creating net supersaturated conditions during the day and hypoxic water column conditions during the nighttime (Figures 4, 6).

*In situ*, the water column was characterized by a vertically stable oxygen concentration without gradients (Figures 4, 7, 8). Gradients were spatially restricted to the benthic microalgae layer and the water-atmosphere interface, and did not extend into the water column. The lack of gradients building up from the bottom indicates that the water column is well-mixed. This was likely facilitated by a combination of wind-driven mixing and turbulence from actively swimming fauna in the ponds.

The water column oxygen concentration varied over the course of the day, spanning more than an order of magnitude. However, even though the oxygen dynamics was proven to be tightly coupled to light availability in the laboratory experiments (Figure 5), *in situ*, the daily temporal oxygen variation was skewed compared to the daily variation in light availability (Figure 6), indicating that other factors also influenced the oxygen variation in the ponds. In the morning, oxygen increased rapidly from 33 to  $638 \mu\text{mol L}^{-1}$  within a short 5-h period, but reached the maximum oxygen concentration at 10:00 at a light intensity of  $\sim 1,000 \mu\text{mol m}^{-2} \text{s}^{-1}$  PAR, approximately

3 h before the light intensity reached its maximum (Figure 6). This rapid increase was also reflected in the morning oxygen profiles, where the water column oxygen increased continuously in four consecutively measured profiles (Figure 4). Subsequently, the oxygen concentration decreased slowly for more than 12 h over the afternoon and evening (Figure 6). This discrepancy between the oxygen dynamics and light availability can be caused by multiple factors. The oxygen flux from the sediment surface was markedly lower in the afternoon showing a more than 50% reduction in the oxygen export from the microalgae layer to the water column compared to the morning (Figure 4). This was likely due to a combination of factors including photoinhibition and increased respiratory demands at higher temperatures. Furthermore, a recent study has shown that gas exchange via gas bubbles (ebullition) also influences oxygen dynamics in salt marsh tidal ponds (Howard et al., 2018), facilitating a route of oxygen exchange between the sediment surface and the atmosphere that bypasses transport of dissolved oxygen through water column. In the present study, gas bubbles were also observed developing at the sediment water interface. Hence, ebullition, driven by high biological oxygen production and a marked increase in temperature, lowering saturation state of dissolved gases, is expected to have played a role in oxygen exchange lowering both oxygen concentrations in the water column and the peak concentration at the sediment-water interface in the afternoon (Figures 4, 6).

The development of seafoam on the water-surface generated a horizontal variation in the vertical oxygen profiles within the ponds. The seafoam had a marked impact on light penetration to the sediment surface. However, only under the thickest layer of seafoam, where light penetration was almost completely blocked, were the oxygen profiles affected, showing a lower concentration in the water column (Figure 7). This supports the findings of the light dependency study, showing that the benthic microalgae community is able to maintain high oxygen production even under reduced light conditions (Figure 5). The development of seafoam also has an impact on pond ecology. Studies have shown that meiobenthic swimmers in intertidal zones change their behavior in response to the formation of sea foam, accumulating under the foam using it for shading and hiding (Armonies, 1989, 1991). It is possible that the shaded sea foam areas, in addition to providing shade, may also function as a refuge from the highly supersaturated oxygen conditions, which can be toxic to aquatic animals stimulating the generation of free radicals (Sebert et al., 1984; Lushchak and Bagnyukova, 2006).

The characteristic oxygen profiles in light; with highly supersaturated water columns and benthic peaks restricted to microalgae layer at the sediment water interface, were reproducible across ponds (Figure 8). There was some variation in the benthic peak concentrations, penetration depth, and oxygen fluxes, possibly caused by the time lag between measurements, but the water column oxygen concentrations were very similar across ponds (Figure 8). Based on these similar patterns in spatial oxygen distribution across different ponds, the *in situ* profiles described in this study (Figures 4, 5, 7, 8) were found to be generally representative for shallow salt marsh ponds in the area.

## pH and CO<sub>2</sub>

The water column was well-buffered, and despite the intense photosynthetic and respiratory activity changing over the course of day, the pH showed attenuated fluctuations and did not reach extreme values, ranging from 6.2 to 7.1 in the time-series study (Figure 6) and 6.5–7.3 in the *in situ* profiles (Figure 4). pH in the water column followed a similar trend as O<sub>2</sub>, decreasing in the afternoon and increasing in the morning (Figure 6). Increased photosynthetic activity at the sediment-water interface had no direct effect on pH, neither in the *in situ* profiles (Figure 4) nor in response to increasing light conditions (Figure 5). The afternoon *in situ* profiles showed some unusual pH activity at the sediment surface, but the two profiles show opposite trends and no conclusions can be drawn on these observations.

Carbon dioxide (CO<sub>2</sub>) accumulated in the sediment resulting in steep gradients at the sediment-water interface spatially aligned with the benthic O<sub>2</sub> peak. The sediment therefore fulfills an important function in the tidal ponds as a CO<sub>2</sub> reservoir for the benthic primary production as the water column was almost devoid of CO<sub>2</sub> in the afternoon (Figure 4). This supports previous observations from deeper tidal ponds in the same marshes, where Spivak et al. (2018) found a significant DIC efflux from the sediment to the water.

## The Impact of Tidal Flooding on O<sub>2</sub>, pH, and Temperature

Tidal inundation had a high, but short-lived, impact on oxygen and pH (Figure 6), which was restricted to the period of the flooding, which lasted 3 h (16:45–19:45). It is noteworthy that after the flood and even during the peak of the flood, where the water is stagnant, the pond O<sub>2</sub> and pH immediately returned to the previous conditions, showing that the driving factors internally in the pond exert a strong control on the pond biogeochemistry. The impact of flood tides is likely to change at different times of the day, as the difference in oxygen, pH, and temperature between tidal water and pond water may be different.

## Differences Between *in situ* and Laboratory Profiles

In the field, the benthic oxygen peaks were restricted to the layer of benthic microalgae. In the laboratory investigations, the benthic oxygen peak extended slightly higher into the water column (Figures 4, 5, note the different y-axis scales). This was likely caused by the less excessive artificial stirring of the water column in the laboratory, increasing the DBL thickness, and partly by differences in the visual determination of the sediment-water interface. In the laboratory, the sediment surface could be determined visually close-up from the side of the core. In the field, the visual determination occurred from above and at a distance. This may have resulted in differences in the perception of the location of the sediment-water interface (“depth 0”) between the *in situ* and laboratory investigations.

## Comparison to Other Studies of Oxygen and pH in Salt Marsh Tidal Ponds

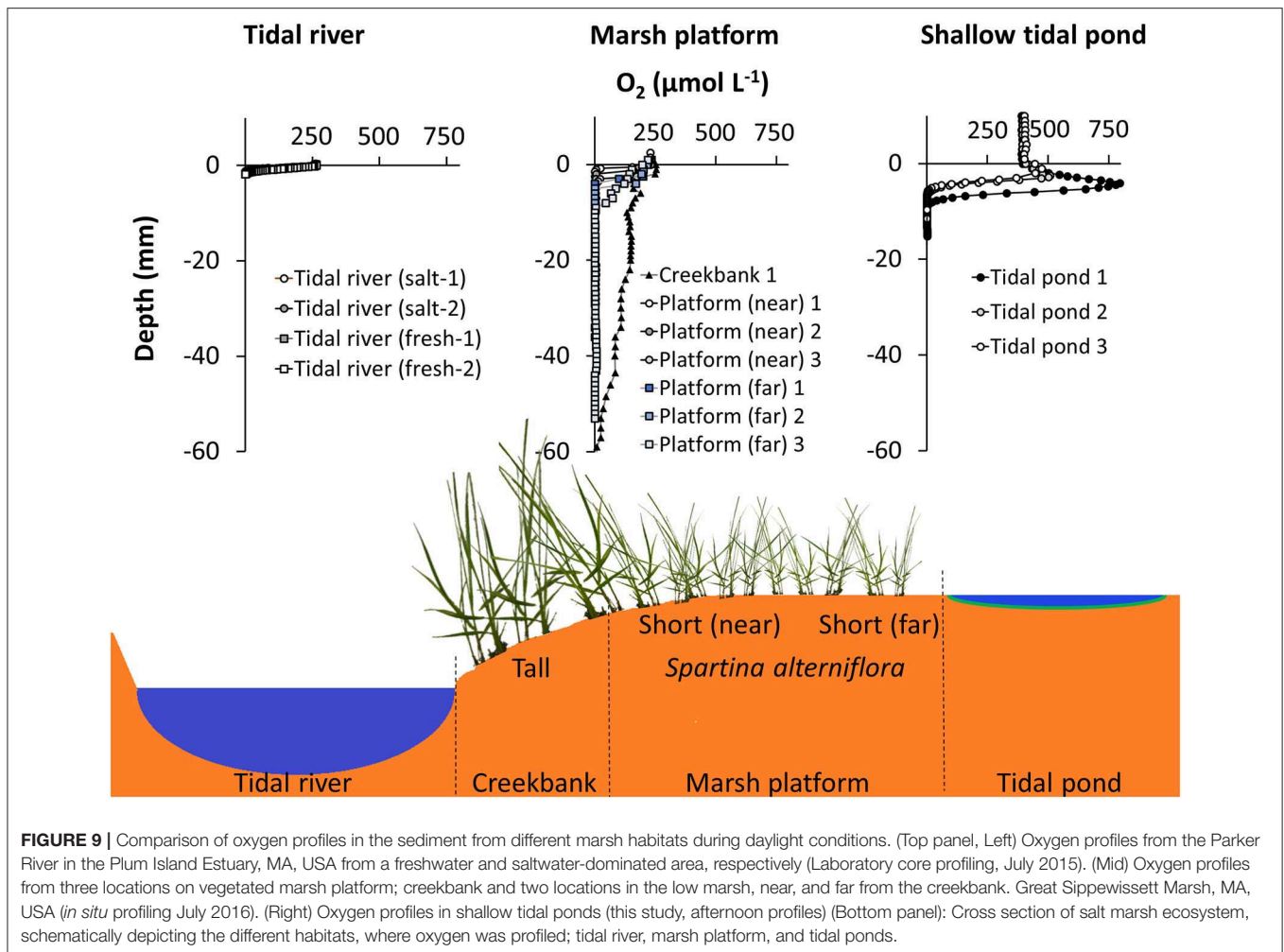
Only a few other studies have investigated oxygen dynamics in salt marsh tidal ponds. In the Plum Island Estuary, where the present study was also conducted, Spivak et al. (2017), investigated the biogeochemistry of the deeper ponds in the area (depth: 25–40 cm) and found the largest oxygen variation in July ranging from supersaturated concentrations of 625 μmol L<sup>-1</sup> at noon to 0 μmol L<sup>-1</sup> in the night time, while the daily variation was lower in the fall. This indicates that the daily oxygen variation also has a seasonal variation and that the oxygen dynamics presented in the current study was measured at the time of the year with the highest oxygen variation. It is noteworthy that Spivak et al. (2017), found the deeper ponds to become anoxic at night, whereas the shallower ponds investigated in the current study reached hypoxic conditions, but did not become anoxic. It is likely that the shallow depth combined with high wind exposure causes mixing that prevents anoxia in the water column. Similar oxygen dynamics were observed in shallower ponds of the Ria de Aveiro salt marshes in Portugal, where Lillebø et al. (2010) found oxygen concentrations to reach a maximum of 250 μmol L<sup>-1</sup> in June, and also here did the oxygen decrease at night, but it did not reach anoxic conditions. In other areas, Salman et al. (2015) measured O<sub>2</sub> profiles in the laboratory on cores from ponds in Sippewissett marsh, Massachusetts, USA, and found marked differences between light and dark conditions. Smith and Able (2003) observed similar diurnal oxygen variation in tidal ponds of New Jersey marshes, with peak concentration in the water column occurring in the late afternoon. These observations are consistent with the findings in the current study.

pH generally shows very attenuated fluctuations in tidal marsh ponds. Lillebø et al. (2010) found small variations around a pH of 7.5 in the Ria de Aveiro salt marshes. Catallo (1999) investigated pH directly at the sediment surface and found very little pH variation at the sediment surface in a Louisiana marsh tidal pond, despite marked changes in water redox potential. These observations of O<sub>2</sub> and pH are consistent with the finding of the present study showing a dynamic oxygen environment with marked swings between day and night, but with well-buffered pH conditions showing only minor pH fluctuations.

In other ponds of the Plum Island Estuary marshes with a depth of ~20 cm, Kearns et al. (2017) demonstrated that short-term changes of environmental conditions can alter the structure of active microbial communities in the water column, whereas the sediment showed low variation of the abiotic environmental conditions and a stable active microbial community. Similar impact on the microbial community is expected to occur in the ponds investigated in the current study. Our detailed profiling of the vertical oxygen distribution revealed a 1 cm layer right around the sediment surface, with the most drastic variation in oxygen. Within this layer, the extreme oxygen variation could have a unique impact on the microbial community, which should be emphasized in future studies.

*In situ* data on oxygen fluxes for salt marsh tidal ponds are lacking in the literature, but the oxygen fluxes measured in





this study were on the same order of magnitude as reported from other marsh habitats. Low marsh sediments showed a net oxygen uptake also during the day time with a net flux of  $0.58 \text{ mmol m}^{-2} \text{ h}^{-1}$  in Nova Scotia marshes (Schwingamer et al., 1991) and  $0.9 \text{ mmol m}^{-2} \text{ h}^{-1}$  in Australian marshes (Brodersen et al., 2019). In tidal marsh creeks, oxygen uptake rates were found ranging from 0 to  $3.2 \text{ mmol O}_2 \text{ m}^{-2} \text{ h}^{-1}$  (Macpherson et al., 2007). In comparison, the oxygen fluxes of shallow tidal ponds are markedly more dynamic and driven by photosynthetic activity of the benthic microalgae, which resulted in oxygen fluxes out of the sediment in the daytime and oxygen uptake at night. In this way, the oxygen dynamics in shallow tidal ponds more resembles the oxygen dynamics found on intertidal flats (Magalhães et al., 2002; Denis and Desreumaux, 2009; Jansen et al., 2009).

The tidal pond oxygen profiles differed markedly from other marsh habitats (Figure 9). In preceding studies also conducted with needle optode profiling under daylight conditions in July of 2015 and 2016, we measured oxygen profiles *in situ* on the vegetated marsh platform of Great Sippewissett Marsh (MA, USA), and in sediment cores from the Parker river in the Plum Island Estuary (MA, USA). On the marsh platform, oxygen penetration was high on creek banks, where drainage is high,

going down to  $\sim 60 \text{ mm}$ , but decreased further up on the platform to  $< 10 \text{ mm}$ , where the sediment is more permanently waterlogged. The sediment surface was air-exposed and the top sediment was always near atmospheric  $\text{O}_2$  concentrations (Figure 9). This is consistent with other studies demonstrating that the typical oxygen profile in the top sediment of the vegetated marsh platform follows a steady decrease from atmospheric saturation at the surface to anoxia within the first 1 cm (Holmer et al., 2002; Brodersen et al., 2019). Below the top 1 cm, the sediment was anoxic on the marsh platform (Figure 9). This is also consistent with previous studies demonstrating that even though the *Spartina*-plants on marsh platform are capable of translocating oxygen and generating oxic root zones (Maricle and Lee, 2002; Koop-Jakobsen et al., 2018), it has limited impact on the bulk rhizosphere sediment that remain anoxic in the summertime (Koop-Jakobsen et al., 2017). In the permanently inundated sediment of the tidal river, the oxygen penetration was very shallow reaching  $< 2 \text{ mm}$  into the sediment, and there was no increased oxygen production at the sediment-water interface. Hence, with the highly supersaturated conditions of the bulk seawater and distinct oxygen peak at the sediment-water interface during the day, the tidal ponds have a markedly different spatial distribution of oxygen compared to other marsh

habitats, and its impact on the microbial community and benthic biogeochemistry needs further attention.

## Perspective

In many North American marshes, tidal ponds are increasing in numbers and areal coverage in response to increased disturbance of the vegetation. A wide range of natural and anthropogenic impacts, including sea-level rise, ditching, and dredging; are contributing to this process (Kirwan et al., 2008; Millette et al., 2010; Wilson et al., 2014; Schepers et al., 2017). Hence, salt marsh tidal ponds may play a more prominent role in salt marsh ecosystems in the future. Consequently, getting a better comprehension of the biogeochemistry in this unique environment is essential for understanding the impact it may have on key ecosystem services; such as nutrient retention and carbon sequestration. Our study demonstrates that tidal ponds comprise a marsh habitat with distinctive spatiotemporal oxygen dynamics driven by benthic respiration and photosynthesis, which is primarily controlled by the light exposure of the sediment surface. These conditions differ from the surrounding vegetated marsh, where the sediment surface is shaded by a vascular plant canopy and directly exposed to the atmosphere. Consequently, an increased coverage of tidal ponds on the vegetated marsh platform is likely to alter the overall salt marsh biogeochemistry; to a system with more dynamic oxygen conditions, switching from high oxygen production at the sediment surface during the day to high oxygen demand at night.

## REFERENCES

- Adamowicz, S. C., and Roman, C. T. (2005). New England salt marsh pools: a quantitative analysis of geomorphic and geographic features. *Wetlands* 25, 279–288. doi: 10.1672/4
- Allen, D. M., Ogburn-Matthews, V., and Kenny, P. D. (2017). Nekton use of flooded salt marsh and an assessment of intertidal creek pools as low-tide refuges. *Estuar. Coasts* 40, 1450–1463. doi: 10.1007/s12237-017-0231-4
- Armonies, W. (1989). Occurrence of meiofauna in *Phaeocystis* seafoam. *Mar. Ecol. Progr. Series* 53, 305–309. doi: 10.3354/meps053305
- Armonies, W. (1991). “Transport of benthos with tidal waters: another source of indeterminism,” in *Report From the Workshop—Modelling the Benthos*, eds P. M. J. Herman, C.H.R. Heip (Yerseke: Delta Institute for Hydrological Research—Royal Netherlands Academy of Arts and Sciences), 11–28.
- Baumann, H., Wallace, R. B., Tagliaferri, T., and Gobler, C. J. (2015). Large natural pH, CO<sub>2</sub> and O<sub>2</sub> Fluctuations in a temperate tidal salt marsh on diel, seasonal, and interannual time scales. *Estuar. Coasts* 38, 220–231. doi: 10.1007/s12237-014-9800-y
- Brodersen, K. E., Trevathan-Tackett, S. M., Nielsen, D. A., Connolly, R. M., Lovelock, C. E., Atwood, T. B., et al. (2019). Oxygen consumption and sulfate reduction in vegetated coastal habitats: effects of physical disturbance. *Front. Mar. Sci.* 6:14. doi: 10.3389/fmars.2019.00014
- Broecker, W. S., and Peng, T. H. (1974). Gas exchange rates between air and sea. *Tellus* 26, 21–35. doi: 10.3402/tellusa.v26i1-2.9733
- Catallo, W. J. (1999). *Hourly and Daily Variation of Sediment Redox Potential in Tidal Wetland Sediments*. Biological Division Science Report USGS/BRD/BSR-1999-0001. U.S. Geological survey.
- Denis, L., and Desreumaux, P.-E. (2009). Short-term variability of intertidal microphytobenthic production using an oxygen microprofiling system. *Mar. Freshw. Res.* 60, 712–726. doi: 10.1071/MF08070
- Harshberger, J. W. (1916). The origin and vegetation of salt marsh pools. *Proc. Am. Philos. Soc.* 55, 481–484.
- Holmer, M., Gribsholt, B., and Kristensen, E. (2002). Effects of sea level rise on growth of *Spartina anglica* and oxygen dynamics in rhizosphere and salt marsh sediments. *Mar. Ecol. Progr. Series* 225, 197–204. doi: 10.3354/meps225197
- Howard, E. M., Forbrich, I., Giblin, A. E., Lott Iii, D. E., Cahill, K. L., and Stanley, R. H. R. (2018). Using noble gases to compare parameterizations of air-water gas exchange and to constrain oxygen losses by ebullition in a shallow aquatic environment. *J. Geophys. Res.* 123, 2711–2726. doi: 10.1029/2018JG004441
- Jansen, S., Walpersdorf, E., Werner, U., Billerbeck, M., Böttcher, M. E., and De Beer, D. (2009). Functioning of intertidal flats inferred from temporal and spatial dynamics of O<sub>2</sub>, H<sub>2</sub>S and pH in their surface sediment. *Ocean Dynam.* 59, 317–332. doi: 10.1007/s10236-009-0179-4
- Kearns, P. J., Holloway, D., Angell, J. H., Feinman, S. G., and Bowen, J. L. (2017). Effect of short-term, diel changes in environmental conditions on active microbial communities in a salt marsh pond. *Aquat. Microb. Ecol.* 80, 29–41. doi: 10.3354/ame01837
- Kirwan, M. L., Murray, A. B., and Boyd, W. S. (2008). Temporary vegetation disturbance as an explanation for permanent loss of tidal wetlands. *Geophys. Res. Lett.* 35:L05403. doi: 10.1029/2007GL032681
- Koop-Jakobsen, K., Fischer, J., and Wenzhöfer, F. (2017). Survey of sediment oxygenation in rhizospheres of the saltmarsh grass - *Spartina anglica*. *Sci. Total Environ.* 589, 191–199. doi: 10.1016/j.scitotenv.2017.02.147
- Koop-Jakobsen, K., Mueller, P., Meier, R. J., Liesch, G., and Jensen, K. (2018). Plant-sediment interactions in salt marshes—an optode imaging study of O<sub>2</sub>, pH, and CO<sub>2</sub> gradients in the rhizosphere. *Front. Plant Sci.* 9:541. doi: 10.3389/fpls.2018.00541
- Lillebø, A. I., Vålega, M., Otero, M., Pardal, M. A., Pereira, E., and Duarte, A. C. (2010). Daily and inter-tidal variations of Fe, Mn and Hg in the water column of a contaminated salt marsh: Halophytes effect. *Estuar. Coast. Shelf Sci.* 88, 91–98. doi: 10.1016/j.ecss.2010.03.014

## DATA AVAILABILITY STATEMENT

The datasets generated for this study are available on request to the corresponding author.

## AUTHOR CONTRIBUTIONS

KK-J conceived this research idea, designed the experiment, conducted the research, analyzed the data, and wrote the manuscript. MG conducted the flux analysis and contributed to method development, data analysis, and manuscript writing. Both authors have approved the manuscript.

## FUNDING

For KK-J, this research was supported by MARUM—Center for Marine Environmental Sciences, University of Bremen, Germany. MG was funded by the PreSens GmbH.

## ACKNOWLEDGMENTS

We thank the Plum Island Ecosystems LTER (NSF-OCE 1637630) and the Ecosystems Center at the Marine Biological Laboratory in Woods Hole, MA, USA, for hosting this study, and we thank the researchers at the *Marshview* and *Rowley-house* field stations for helping out with the logistics of the fieldwork.

- Lushchak, V. I., and Bagnyukova, T. V. (2006). Effects of different environmental oxygen levels on free radical processes in fish. *Compar. Biochem. Physiol. B* 144, 283–289. doi: 10.1016/j.cbpb.2006.02.014
- Mackenzie, R. A., and Dionne, M. (2008). Habitat heterogeneity: importance of salt marsh pools and high marsh surfaces to fish production in two Gulf of Maine salt marshes. *Mar. Ecol. Progr. Series* 368, 217–230. doi: 10.3354/meps07560
- Macpherson, T. A., Cahoon, L. B., and Mallin, M. A. (2007). Water column oxygen demand and sediment oxygen flux: patterns of oxygen depletion in tidal creeks. *Hydrobiologia* 586, 235–248. doi: 10.1007/s10750-007-0643-4
- Magalhães, C. M., Bordalo, A. A., and Wiebe, W. J. (2002). Temporal and spatial patterns of intertidal sediment-water nutrient and oxygen fluxes in the Douro River estuary, Portugal. *Mar. Ecol. Progr. Series* 233, 55–71. doi: 10.3354/meps233055
- Maricle, B. R., and Lee, R. W. (2002). Aerenchyma development and oxygen transport in the estuarine cordgrasses *Spartina alterniflora* and *Spartina anglica*. *Aquat. Botany* 74, 109–120. doi: 10.1016/S0304-3770(02)00051-7
- Millette, T. L., Argow, B. A., Marcano, E., Hayward, C., Hopkinson, C. S., and Valentine, V. (2010). Salt marsh geomorphological analyses via integration of multitemporal multispectral remote sensing with LIDAR and GIS. *J. Coast. Res.* 26, 809–816. doi: 10.2112/JCOASTRES-D-09-00101.1
- Raposa, K. B. (2008). Early ecological responses to hydrologic restoration of a tidal pond and salt marsh complex in Narragansett Bay, Rhode Island. *J. Coast. Res.* 180–192. doi: 10.2112/SI55-015
- Raposa, K. B., and Roman, C. T. (2001). Seasonal habitat-use patterns of nekton in a tide-restricted and unrestricted New England salt marsh. *Wetlands* 21, 451–461. doi: 10.1672/0277-5212(2001)021<0451:SHUPON>2.0.CO;2
- Ruber, E., Gillis, G., and Montagna, P. A. (1981). Production of dominant emergent vegetation and of pool algae on a Northern Massachusetts Salt Marsh. *Bull. Torrey Bot. Club* 108, 180–188. doi: 10.2307/2484897
- Salman, V., Yang, T., Berben, T., Klein, F., Angert, E., and Teske, A. (2015). Calcite-accumulating large sulfur bacteria of the genus *Achromatium* in Sippewissett Salt Marsh. *Isme J.* 9:2503. doi: 10.1038/ismej.2015.62
- Schepers, L., Kirwan, M., Guntenspergen, G., and Temmerman, S. (2017). Spatio-temporal development of vegetation die-off in a submerging coastal marsh. *Limnol. Oceanogr.* 62, 137–150. doi: 10.1002/lno.10381
- Schwinghamer, P., Kepkay, P. E., and Foda, A. (1991). Oxygen flux and community biomass structure associated with benthic photosynthesis and detritus decomposition. *J. Exp. Mar. Biol. Ecol.* 147, 9–35. doi: 10.1016/0022-0981(91)90034-T
- Sebert, P., Barthelemy, L., and Peyraud, C. (1984). Oxygen toxicity in trout at two seasons. *Comp. Biochem. Physiol. A* 78, 719–722. doi: 10.1016/0300-9629(84)90622-4
- Smith, K. J., and Able, K. W. (1994). Salt-marsh tide pools as winter refuges for the mummichog, *Fundulus heteroclitus*, in New Jersey. *Estuaries* 17, 226–234. doi: 10.2307/1352572
- Smith, K. J., and Able, K. W. (2003). Dissolved oxygen dynamics in salt marsh pools and its potential impacts on fish assemblages. *Mar. Ecol. Progr. Series* 258, 223–232. doi: 10.3354/meps258223
- Spivak, A. C., Gosselin, K., Howard, E., Mariotti, G., Forbrich, I., Stanley, R., et al. (2017). Shallow ponds are heterogeneous habitats within a temperate salt marsh ecosystem. *J. Geophys. Res.* 122, 1371–1384. doi: 10.1002/2017JG003780
- Spivak, A. C., Gosselin, K. M., and Sylva, S. P. (2018). Shallow ponds are biogeochemically distinct habitats in salt marsh ecosystems. *Limnol. Oceanogr.* 63, 1622–1642. doi: 10.1002/lno.10797
- Weiss, R. F. (1970). The solubility of nitrogen, oxygen and argon in water and seawater. *Deep Sea Res. Oceanogr. Abstr.* 17, 721–735. doi: 10.1016/0011-7471(70)90037-9
- Whitney, D. E., and Darley, W. M. (1983). Effect of light intensity upon salt marsh benthic microalgal photosynthesis. *Mar. Biol.* 75, 249–252. doi: 10.1007/BF00406009
- Wilson, C. A., Hughes, Z. J., Fitzgerald, D. M., Hopkinson, C. S., Valentine, V., and Kolker, A. S. (2014). Saltmarsh pool and tidal creek morphodynamics: Dynamic equilibrium of northern latitude saltmarshes? *Geomorphology* 213, 99–115. doi: 10.1016/j.geomorph.2014.01.002
- Yuan-Hui, L., and Gregory, S. (1974). Diffusion of ions in sea water and in deep-sea sediments. *Geochim. Cosmochim. Acta* 38, 703–714. doi: 10.1016/0016-7037(74)90145-8

**Conflict of Interest:** The sensor company, PreSens Precision Sensing GmbH, Regensburg, Germany, provided the needle optode profiling equipment for this study. PreSens GmbH had no restrictive rights in regards to this publication beyond those entitled by their Co-Authorship. All final decisions on the content of this manuscript was solely the responsibility of KK-J.

The remaining author declares that the research was conducted in the absence of any commercial or financial relationships that could be construed as a potential conflict of interest.

Copyright © 2019 Koop-Jakobsen and Gutbrod. This is an open-access article distributed under the terms of the Creative Commons Attribution License (CC BY). The use, distribution or reproduction in other forums is permitted, provided the original author(s) and the copyright owner(s) are credited and that the original publication in this journal is cited, in accordance with accepted academic practice. No use, distribution or reproduction is permitted which does not comply with these terms.